Balint, Roland; Engblom, Markus; Niemi, Jonne; Lindberg, Daniel; Saarinen, Timo; Rautala, Jaakko; Hupa, Mikko; Hupa, Leena

Morphological and chemical differences within superheater deposits from different locations of a black liquor recovery boiler

Published in:
Energy

DOI:
10.1016/j.energy.2022.126576

Published: 15/03/2023

Document Version
Publisher's PDF, also known as Version of record

Please cite the original version:
Balint, R., Engblom, M., Niemi, J., Lindberg, D., Saarinen, T., Rautala, J., Hupa, M., & Hupa, L. (2023). Morphological and chemical differences within superheater deposits from different locations of a black liquor recovery boiler. *Energy*, *267*, Article 126576. https://doi.org/10.1016/j.energy.2022.126576

Energy 267 (2023) 126576

Contents lists available at ScienceDirect

Energy

journal homepage: www.elsevier.com/locate/energy

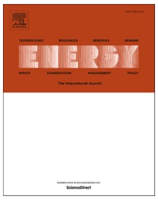

Morphological and chemical differences within superheater deposits from different locations of a black liquor recovery boiler

Roland Balint [a,*], Markus Engblom [a], Jonne Niemi [a], Daniel Lindberg [b], Timo Saarinen [c], Jaakko Rautala [c], Mikko Hupa [a], Leena Hupa [a]

[a] *Johan Gadolin Process Chemistry Centre, Åbo Akademi University, Turku, Finland*
[b] *Department of Chemical and Metallurgical Engineering, Aalto University, Espoo, Finland*
[c] *Metsä-Fibre Oy, Rauma, Finland*

ARTICLE INFO

Handling Editor: Henrik Lund

Keywords:
Superheater deposits
Temperature gradient
Ageing mechanism
Local melting behaviour

ABSTRACT

The effects of two deposit ageing mechanisms were identified by analysing superheater ash deposits from a kraft recovery boiler. Local differences in deposit morphology and chemical composition were identified under the electron microscope. Temperature-gradient-induced diffusion of alkali chloride vapours toward the steel was evident. Two deposit types were identified, based on local chemical compositions: "Type 1" deposits had an innermost porous layer of fine, sintered fume particles enriched in K and Cl, that deposited after homogeneous condensation in the gas phase. "Type 2" deposits formed via sulfation of initially deposited fume particles rich in K and Cl. Thus the innermost layer was enriched in K and S, while concurrently depleted in Cl. Differences in the local first melting temperature (T_0) within the innermost regions of the two deposit types were identified. T_0 reached a minimum within the innermost region of Type 1 deposits, implying an increased risk for melt formation and corrosion. Whereas for Type 2 deposits, T_0 was increased closest to the steel, reducing the risk for melt formation and superheater corrosion. The presented results provide a better understanding of intra-depositional changes taking place after initial deposition, helping assess risks of deposit-related operational problems in the boiler.

1. Introduction

About 90% of chemical pulp worldwide is produced via the kraft pulping process, making it the most used process in the industry [1]. A pulp fibre yield of up to 55% can be achieved, by dissolving wood in an aqueous solution of Na_2S and NaOH [1]. The mixture of spent pulping chemicals, dissolved organic matter from the wood, and water is referred to as black liquor. In large-scale industrial steam boilers, the kraft recovery boilers, black liquor is burned to produce heat and power but also to recover the spent pulping chemicals. Recovery rates of the spent pulping chemicals reach values of up to 98%, eliminating the need for new chemicals almost completely [2]. At the same time, the power produced in a modern kraft recovery boiler typically exceeds the mill's energy needs [2]. In Finland, the pulp and paper industry is a vital part of both economy and national energy supply, as 86% of the country's land area is covered by forest [3]. In 2020 renewable energy was the largest energy source in Finland, supplying 40% of the country's energy demand [3], whereof around one-third is produced from black liquor combustion [3].

Compared to other biofuels, black liquor contains higher amounts of inorganic compounds originating mainly from pulping chemicals, but also raw wood [4]. During combustion, parts of these inorganic compounds are released into the gas phase, forming ash deposits on heat exchanger surfaces in the colder parts of the boiler. Such deposits contain predominantly Na_2SO_4, Na_2CO_3, NaCl, Na_2S and their K counterparts [5]. Na and S originate mainly from the pulping chemicals, while K and Cl originate mainly from wood [4]. Thus, the composition of ash deposits in kraft recovery boilers is affected by the wood type used in the pulping process. Both K and Cl can cause severe operational issues in the boiler, affecting the melting behaviour of ash deposits significantly [5,6]. An increased K content lowers the first melting temperature (T_0) of a deposit [5], while an increase in deposit Cl increases the amount of melt formed at T_0 [6].

The initial formation and build-up of ash deposits in recovery boilers

---

[*] Corresponding author. Laboratory of Molecular Science and Engineering, Faculty of Science and Engineering (FNT), Åbo Akademi University, Henriksgatan 2, Åbo, FI-20500, Finland.

E-mail address: roland.balint@abo.fi (R. Balint).

https://doi.org/10.1016/j.energy.2022.126576
Received 18 July 2022; Received in revised form 8 November 2022; Accepted 27 December 2022

have been studied thoroughly over the last decades and are well understood by now [7,8]. Three particle size fractions have been identified to contribute to the formation of deposits in kraft recovery boilers [9]. The first layer of superheater deposits formed in kraft recovery boilers consists of submicron-sized fume particles, typically enriched in K and Cl, forming a sticky deposit layer and enabling deposition of larger intermediate-sized and carry-over particles, accelerating the deposit growth rate.

More recent experimental data have shown ash deposits to undergo changes in their local chemical composition and morphology, after their initial formation, referred to as deposit ageing [10–12]. These processes are less understood and over the last years, deposit ageing mechanisms have been studied under well-controlled conditions on a laboratory scale at Åbo Akademi University [10–12]. Three different deposit ageing mechanisms have been identified when exposing synthetic ash deposits to a temperature gradient [10,11]. Deposit ageing has been identified to cause densification of ash deposits, increasing the tensile adhesion strength [13], thus hampering removal via sootblowing. Furthermore, local enrichment of corrosive compounds toward the steel has been identified to take place via several pathways [11,12].

Despite ash deposition, and operational problems connected to it, have been studied extensively over the last decades, no data on systematic deposit ageing studies of actual superheater deposits can be found in the literature. A change from laboratory experiments to full-scale deposit studies provides additional valuable information. Not only do full-scale data help in confirming earlier findings from laboratory experiments, carried out under well-controlled conditions. But scaling up to actual boiler conditions also provides additional information on other experimental parameters, which have not been possible to be simulated in the laboratory. Among these parameters are e.g. the impact of sootblowers, reactions between the formed deposit and the flue gas, or continuous deposition of new material and concurrently occurring deposit ageing reactions.

Studies utilising full-scale deposits focused mainly on deposit sintering [14,15], or the initial deposit build-up by carrying out short-term probe measurements [16,17]. However, a few examples indicating deposit ageing to be also of relevance for actual ash deposits in steam power boilers were found in the literature [18,19]. Several studies reported the formation of a layered deposit structure, which typically has been associated with changes in the operating conditions of the boiler or governing deposition mechanisms [8,18,20,21]. Reeve et al. [8] have analysed deposits collected on an air-cooled probe and identified local enrichment in K and Cl within the deposit, toward the steel surface. The observed enrichment has been concluded to be the result of alkali chloride vapours in the flue gas penetrating the outer sintered deposit layer through cracks and subsequently condensing in the inner parts of the deposit. Other studies have identified the local enrichment in S due to sulfation of alkali chlorides [7] and carbonates [22] to be of relevance for kraft recovery boiler deposits, causing melt formation due to compositional changes within the deposit. Sulfation of deposits has also been identified in several straw-fired boilers [18] after the deposits had formed on the superheater tubes. A more recent study carried out in a Brazilian kraft recovery boiler [20] has identified clear enrichment in Cl and K within the region of the deposit closest toward the steel, resulting in a local decrease in the first melting temperature of the deposit and severe melt-induced corrosion of the superheater tubes. In a separate study, deposit samples of this same Brazilian boiler have been analysed in more detail regarding their deposit ageing behaviour [23]. All three ageing mechanisms previously seen within laboratory experiments have also been identified within these actual superheater deposits. Furthermore, a local decrease in T_0 due to local K enrichment connected to deposit ageing has been identified within these deposits [23]. However, more work is needed to better understand and possibly predict deposit ageing mechanisms in actual superheater deposits of boilers.

The objective of the present work was to shed more light on the role of temperature gradient-induced deposit ageing by detailed characterization of deposit samples from a Finnish kraft recovery boiler. Deposit samples were collected from eight locations within the superheater region during a shutdown of the boiler. Cross-sections of the deposit samples were analysed using scanning electron microscopy and energy dispersive X-ray analysis (SEM/EDX). Several differences in deposit morphology, chemistry, and local melting behaviour among the analysed samples were observed, and different deposit types were identified. These differences are expected to affect the deposit's corrosiveness and removability to different extents.

2. Methods

The present study analysed kraft recovery boiler superheater deposits using SEM/EDX. The deposits were obtained directly from tertiary superheater tubes of a kraft recovery boiler located in Rauma, Finland. The boiler's maximum firing capacity is 3200 tonnes of dry solids per day. The superheater tubes were accessed through eight manholes in the boiler wall, four on each side of the boiler. The exact sampling locations are shown in Fig. 1.

Four sampling locations (L1, L2, R1, and R2) were situated in the upper region of the superheater, close to the boiler roof, and four sampling locations (L3, L4, R3, and R4) were situated in the lower region of the superheater tubes, close to the bull-nose. Deposits were directly scraped off the superheater tubes during a boiler shutdown in September 2019. However, the exact orientation of the analysed deposits concerning their direction to the flue gas stream (wind-side, lee-side, or somewhere between) was not known. Before the shutdown, the boiler had been operating continuously for about 30 days. The fired black liquor had a dry solids content of 74%. The composition of the as-fired black liquor and reference values for a black liquor composition typical for northern Europe are given in Table 1. The oxygen content shown in the table is determined by closing the mass balance.

The steam temperature in the tertiary superheater of the boiler in question averages 480 °C during regular operation. The recovery boiler is not equipped to measure the flue gas temperature in the superheater region from which the samples were obtained. Flue gas temperatures in the region of the boiler the samples were taken from typically range between 600 and 650 °C.

For a detailed analysis of the local chemical composition, the deposit samples were cast in epoxy resin to prevent any loss of deposit material during further processing of the samples. The cast deposits were then cut to obtain a cross-section, which was polished using SiC polishing paper. No additional lubricants were used during sample preparation to avoid the dissolution of the water-soluble deposit. The polished deposit cross-sections were cleaned using petroleum ether, and subsequently carbon-coated. The general morphology and chemical composition throughout the deposit cross-sections were analysed using scanning electron microscopy (SEM) and energy dispersive X-ray (EDX) analysis (LEO Gemini 1530 equipped with a ThermoNORAN Vantage X-ray analysing system manufactured by Thermo Scientific), operated at an accelerating voltage of 20 kV and a working distance of 13 mm. Backscatter SEM images were used to obtain morphological information and EDX data was used to analyse the chemical composition of the deposits. The molar fractions of Na, K, Cl, and S were obtained directly from EDX analysis. The C content of the deposits was subsequently calculated by closing the charge balance. The O content was calculated by assuming all C was present as carbonate and all S as sulfate.

Based on the results from SEM/EDX analysis, the local first melting temperature of the deposits was calculated. Each cross-sectional SEM image was divided into various sections, based on local differences in the chemical composition. For each of these sections, the average composition was calculated, which was then utilised to calculate the respective T_0 of the section. T_0 calculations were carried out using FactSage Version 8.1 [25] and the FTPulp thermodynamic database [26], containing data relevant for salt mixtures containing NaCl, KCl, Na_2SO_4, K_2SO_4, Na_2CO_3, K_2CO_3, Na_2S, and K_2S typical for deposits occurring in

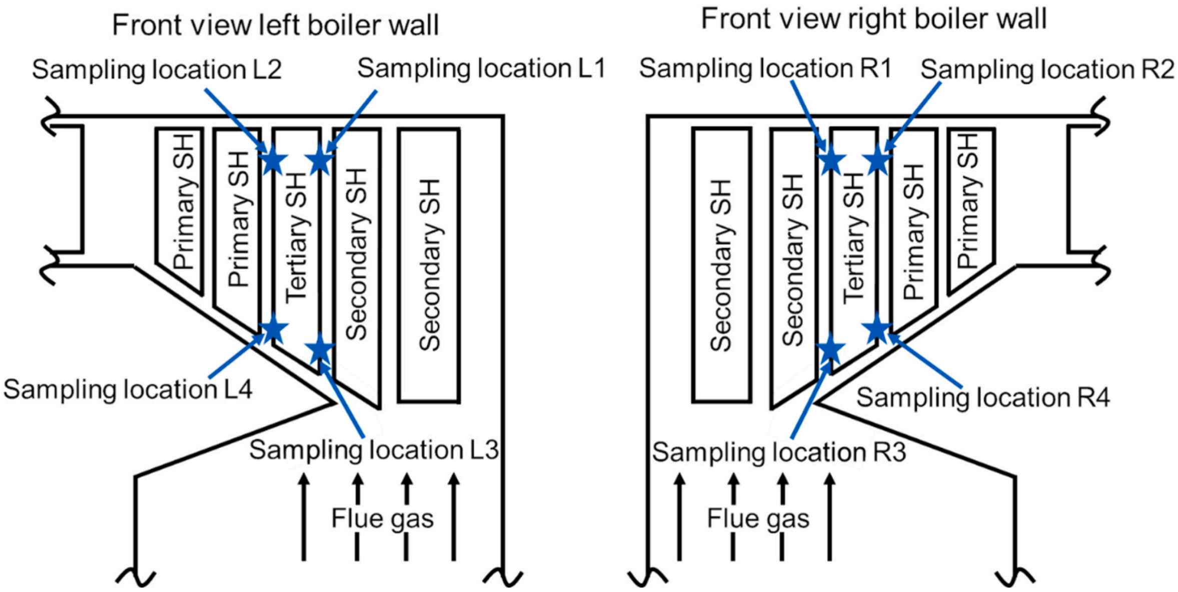

Fig. 1. Schematic front view drawing of left and right side of the superheater area of the boiler with the deposit sampling locations at the tertiary superheater tube bundle indicated.

Table 1
Composition of the black liquor "as-fired" utilised in the present study and reference values of typical black liquor composition in northern Europe.

Element [wt-%]	Black liquor fired in present study	Typical black liquor composition in northern Europe [24]
C	32.8	29.4
H	3.7	3.7
N	0.1	0.2
S	5.7	3.2
Na	20.4	20.8
K	2.8	1.5
Cl	0.3	0.5
O	34.1	40.5
Others	0.1	0.2

kraft recovery boilers. The following phases were considered in the calculation: Liquid phase (designated as FTpulp-MELTA in FactSage); high-temperature, hexagonal alkali sulfate-carbonate solid solution (FTpulp-Hexa); several low-temperature alkali sulfate-carbonate solid solutions (FTpulp-KCO; FTpulp-NKCB; FTpulp-NKCA; FTpulp-OrtA; FTpulp-OrtB); alkali chloride solid solution (FTpulp-ACL); alkali sulfide solid solution (FTpulp-NAKS); and glaserite ($K_3Na_2(SO_4)_2$-based solid solution, FTpulp-Gsrt). In all calculated cases, only the hexagonal phase and alkali chloride were the solid phases stable at T_0 of the system. Using this method, the impact of local elemental enrichment on the deposit's local first melting temperature was studied.

3. Results and discussion

3.1. General deposit characteristics

A total of 13 deposits were analysed regarding their chemical composition and morphology. Morphological differences between individual deposits were identified. The main morphological features are presented in the following paragraph. Fig. 2 shows SEM images of selected deposit cross-sections from various sampling locations.

All SEM images of deposit cross-sections shown in Fig. 2 and the following figures are oriented in the same way. The deposit surface at the bottom of the image was closest to the superheater steel during boiler operation while the deposit surface at the top of the image was facing the flue gas. Thus the local temperature throughout the deposit cross-section increases from the bottom of the image toward the top, due to the temperature difference between the cool superheater steel and the hotter flue gas. However, the orientation of the images in Fig. 2 does not correspond to the actual orientation in the boiler, as the superheater tubes are vertically aligned in the boiler.

As shown in Fig. 2, all analysed deposits were sintered but to a varying degree of porosity. The Cl content suggests that the amount of melt formed in the deposits during boiler operation was relatively low. Thus, the deposits remained porous as the amount of melt was not sufficient for liquid phase sintering, not even toward the outer deposit surface where the local temperatures were the highest. Clear morphological differences between deposits from sampling points 1 and 2 (Fig. 2 A and B), close to the boiler roof, and deposits from sampling points 3 and 4 (Fig. 2C, D, and E), close to the bullnose, were identified.

Deposits from the upper superheater region can be divided into two distinct regions. The innermost layer typically consisted of small particles that sintered into a well-connected skeletal network (Fig. 2 G). With increasing distance to the steel, the deposit morphology changed and the sintered agglomerates increased in size (Fig. 2 F). A more detailed description of these two layers and their underlying formation mechanisms are presented in the further course of the text.

Deposits from the lower superheater region typically contained irregularly shaped particles, significantly larger than the sintered agglomerates on the outer region of deposits from sampling locations one and two (Fig. 2H). The originally deposited particles could still be identified. Deposits from the lower superheater region did not form a skeletal structure. The exact formation mechanism of the deposits from the lower superheater region is not fully understood. However, the morphological features suggest formation via deposition of larger carryover particles, which were partially molten in flight, thus adhered on the superheater tubes, and solidified after impaction. The proposed deposition mechanism accounts for the low porosity of deposits from the lower superheater region. As the deposits did not form a dense molten layer but contained gaps between the single particles, liquid phase sintering was ruled out to have taken place within deposits from the lower superheater region.

Also among samples from the same sampling point, especially the lower superheater region, significant differences in deposit morphology were seen (Fig. 2 D and E). The exact formation mechanisms resulting in the seen morphological differences are currently not understood, and further research is needed.

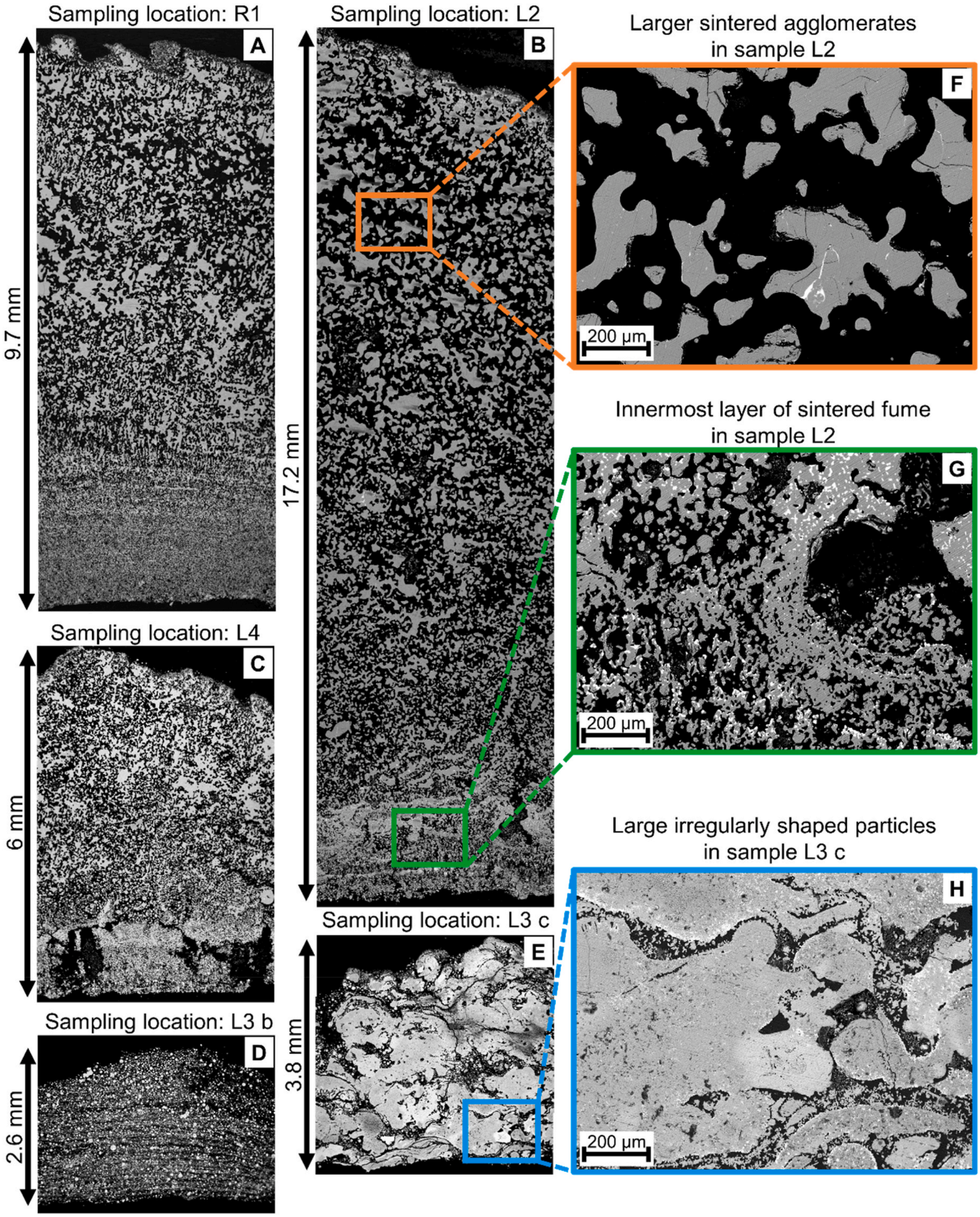

Fig. 2. Selected SEM images of deposit cross-sections from upper superheater region (A and B) and lower superheater region (C, D, and E); zoomed images (F, G, and H) highlighting the main morphological differences between samples; different shades of grey representing the deposit material and black regions corresponding to gas phase (epoxy resin). (For interpretation of the references to colour in this figure legend, the reader is referred to the Web version of this article.)

Besides morphological differences, the deposits from the lower superheater region were typically thinner, with an average thickness of 5.9 mm, compared to deposits from the upper superheater region with an average thickness of 19.6 mm. Multiple parameters can have an impact on the deposit thickness during boiler operation. The distance to the closest sootblower and frequency of sootblowing can account for significant differences within the final deposit thickness as well as the particle load in the flue gas. The bulk of the flue gas enters the upper superheater region after exiting the furnace, resulting in a higher particle load within the region of the upper superheater tubes (sampling points 1 and 2) compared to the lower superheater region (sampling points 3 and 4) close to the bull-nose. It has been shown for the deposition rate increases linearly with increasing particle load [27]. Thus, the deposit build-up rate was expected to be higher in the upper superheater region compared to the lower superheater region.

For further detailed analysis in the present report, only deposits collected from the upper superheater region were utilised. This allowed for easier comparison between the present deposit samples and superheater deposits from the upper superheater region of a Brazilian kraft recovery boiler, presented elsewhere [23].

Despite the differences in deposit morphologies seen in Fig. 2, no significant variations in the bulk composition among all analysed deposits were observed. The calculation of the average bulk deposit composition of all analysed deposits was based on EDX data of the cross-sections. In Table 2, the mass-based average bulk deposit composition of all obtained deposits is shown.

The bulk deposit composition in Table 2 was calculated by assuming that all sulfur was bound as sulfate. The carbonate content was calculated by closing the charge balance. The main constituents of the deposits were Na and SO_4, making up almost 78 wt-% of the deposit, while Cl made up 0.7 wt-% on average. The Cl content in the Finnish deposit samples was lower compared to Brazilian superheater deposits [23]. In general, superheater deposits from Scandinavian and also North American kraft recovery boilers have a lower Cl content than deposits from South America due to the wood type used in the pulping process [4]. This difference in deposit Cl content is thought to be mainly responsible for the differences in deposit morphology between the Finnish and Brazilian deposits.

Due to the low deposit Cl content, no significant melt formation was expected within the deposits at the prevailing flue gas temperatures. The calculated melting curve based on the average deposit composition (Table 2) also suggested a low amount of melt to form at the expected maximum flue gas temperature as shown in Fig. 3.

The amount of melt formed at T_0 was very low, 2 wt-%, and did not increase significantly with increasing temperature. Up to 675 °C, i.e., above the estimated maximum flue gas temperature at the sampling location, the amount of melt within the deposit remained below 10 wt-%. Only at temperatures above 725 °C, well above temperatures relevant for the present deposit samples, the formed amount of melt began to increase more steeply.

Even though no significant differences in the average deposit composition between single samples were seen, local enrichment of elements such as Cl, K and S were observed in SEM/EDX analyses. Two main enrichment patterns were identified, thus the deposits were classified into two main deposit types based on their local chemical composition in the region closest to the steel. In the following, the main characteristics of the two deposit types from the upper superheater region are presented.

3.2. Initial deposit layer of fume enriched in K and Cl – “type 1” deposit

The first deposit type, “Type 1”, can be divided into three distinct regions as shown in Fig. 4.

Closest to the steel (Fig. 4 A), the deposit consisted of a porous layer of a network of fine, sintered particles. A similar morphology has also been identified in laboratory studies investigating the condensation of alkali chloride vapours from hot flue gases onto cold steel tubes [28,29], as well as in deposition experiments burning black liquor in an entrained flow reactor [30]. The observed morphology of fine sintered particles was suggested to have resulted from homogeneous condensation of alkali chlorides in the gas phase. The condensation products were then transported to the steel surface through the thermal boundary layer via thermophoresis and subsequently deposited on the cold steel surface [28,29].

Table 2
Mass-based average bulk composition of all deposits obtained in wt-%.

Component	Mass fraction [wt-%]
Na	31.9
K	4.6
Cl	0.7
SO_4	45.7
CO_3	17.1

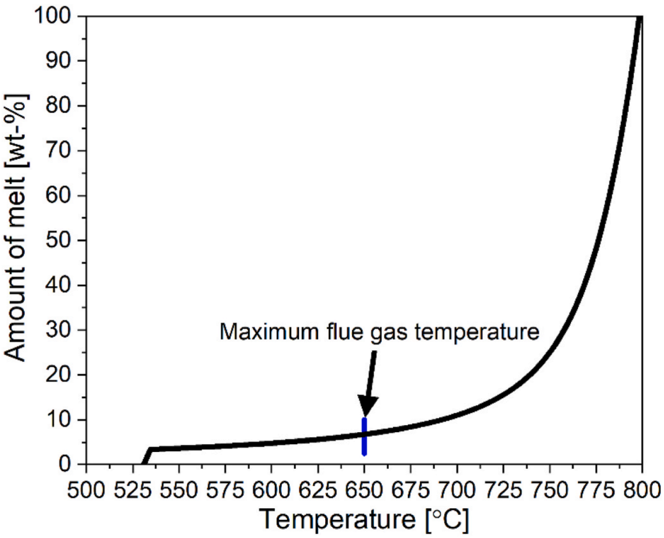

Fig. 3. Melting behaviour of average bulk deposit composition given in Table 2. Estimated maximum flue gas temperature at the sampling location indicated.

In the context of recovery boilers, condensation products forming in the flue gas are called fume, typically forming an initial sticky deposit layer on the superheater tubes. Fume particles are of sub-micrometre size and enriched in alkali chlorides [15]. During black liquor combustion, inorganic compounds are released into the flue gas, with alkali chlorides having higher vapour pressures compared to alkali carbonate, sulfate, and sulfide. Therefore, larger amounts of alkali chloride vaporise and enrich in the flue gas. In the superheater region, the inorganic vapours condense as the temperature decreases. These condensation products are not only enriched in Cl due to the higher volatility of alkali chlorides but additionally, enrichment in K is typically observed, as the volatility of KCl is higher compared to NaCl [31].

Fig. 4 D and E show the molar Cl/(Na + K) and K/(Na + K) ratios within the deposit cross-section. The innermost layer of “Type 1” deposits was enriched in K and Cl compared to the outer regions. Layers enriched in K and Cl parallel to the steel surface were observed throughout the enriched region. However, a more detailed analysis did not show any significant formation of alkali chloride layers on the furnace-facing side of particles, typical for temperature gradient-induced diffusional transport of alkali chloride. Currently, the layered enrichment in alkali chloride is believed to have formed predominantly during initial deposit formation via the above-mentioned condensation mechanism.

Besides differences in the local chemical composition, the particle size within the innermost deposit layer of “Type 1” deposits was significantly smaller compared to the outer regions, as mentioned above. A more detailed analysis of the particle size showed the particle diameter of the innermost layer was slightly below 1 μm on average, implying the main constituent of this region was fume particles [15]. Fume concentration in recovery boiler flue gas streams typically ranges between 10 and 35 g/Nm^3, while the concentration of larger carry-over particles ranges between 2 and 4 g/Nm^3 [24]. Furthermore, the sampling location favours the formation of an initial deposit layer via fume deposition. Carry-over particles deposit via inertial impaction [18]; thus, most larger particles are expected to not reach the tertiary superheater tubes but instead deposit already on the secondary superheater tubes [32]. Therefore, the analysed deposit morphology, chemical composition, and the general understanding of deposit formation in kraft recovery boilers verified the suggested condensation mechanism yielding the innermost

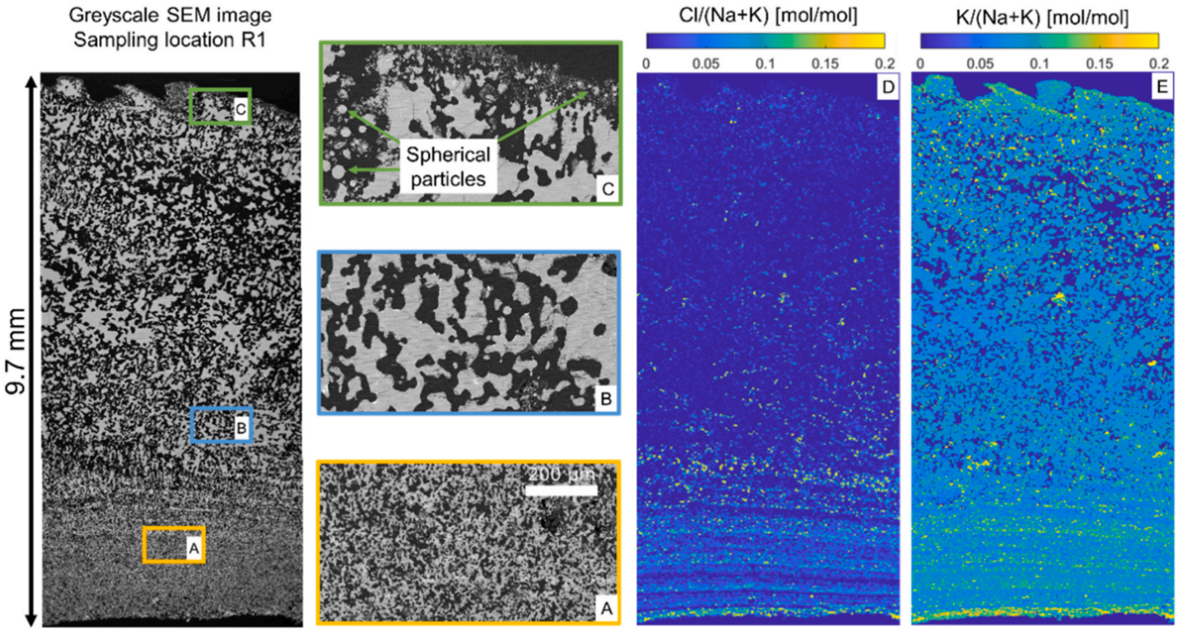

Fig. 4. SEM image of “Type 1″ deposit with A) region of fine sintered particles enriched in K and Cl; B) bulk of larger sintered agglomerates; C) layer of spherical particles on outer deposit surface; D) molar Cl/(Na + K) ratio; and E) molar K/(Na + K) ratio.

layer of “Type 1” deposits.

No indications of melt formation within this innermost region of the deposit during boiler operation were found. Closest to the steel, the local deposit temperature was the lowest and expected to remain below T_0 during boiler operation. The steel temperature of the superheaters is kept at temperatures well below T_0 of the bulk deposit to avoid any melt getting in direct contact with the steel. Even deposits from different boilers, with higher Cl concentrations and higher amounts of melt formed during boiler operation, have been shown to contain a porous layer closest to the steel due to the low local temperatures [23].

It is worth mentioning that, in a few cases, the innermost deposit layer of fine, sintered particles was missing, indicating material loss. As the deposits were mechanically removed from the superheater tubes, it is not clear if material was lost during sampling. Thus, it cannot be ruled out that the innermost layer of fine, sintered particles of some deposit samples was damaged during sampling and transportation, resulting in the lack of the innermost deposit layers. Especially, as the region of fine sintered particles appeared to be more fragile than the remaining deposit toward the hotter outer deposit surface, the lack of the innermost deposit layer is currently believed to be a sampling artefact.

The porous layer consisting of fine, sintered particles seen in Region A in Fig. 4 is followed by a second sintered layer consisting of larger agglomerates (Region B). Within Region B, the local temperature was higher compared to Region A due to the temperature gradient in the deposit. The smooth edges on the irregularly shaped particles indicated the local deposit temperature having been above T_0 during boiler operation, resulting in initial melt formation. However, as shown in Fig. 3, the amount of melt formed was below 10 wt-% throughout the deposit as the flue gas temperature at the sampling location did not exceed 650 °C. The amount of melt was thus insufficient to form a dense molten layer. Similar results have been observed in synthetic deposit samples studied in the laboratory [10–12].

The alkali chloride layers on the furnace-facing side of particles in Region B were more pronounced than in Region A. The gap size between two distinct particles was larger in Region B than in Region A, causing larger temperature differences between two distinct particles in Region B. Subsequently, the concentration gradient of alkali chloride in the gas phase increased, resulting in higher diffusional transport rates. Similar observations of the air gap size affecting the rate of diffusional alkali chloride transport have been reported in laboratory experiments [12]. Thus, the change in deposit morphology was believed to contribute to the increased alkali chloride layer thickness with increasing distance from the steel. Furthermore, higher local temperatures increase the alkali chloride vapour pressure, resulting in a larger concentration gradient of alkali chloride in the gas phase. In comparison to laboratory experiments, the Cl layers were thinner in actual boiler deposits. The observed difference is due to the temperature gradient in the boiler deposits being smaller, resulting in slower transport rates of alkali chloride vapours compared to the laboratory experiments. Furthermore, the boiler deposits contained less alkali chloride, thus the layers could not reach an equal thickness. However, the underlying mechanism of diffusional vapour transport resulting in the formation of such alkali chloride layers is not expected to be further affected when comparing the laboratory set-up to the boiler environment.

Within several of the analysed deposit samples, alkali chloride-rich regions were not exclusively observed on the furnace-facing sides of particles but also within larger sintered agglomerates. The small amount of melt within the deposit is highly enriched in Cl compared to the original deposit. Melt tended to accumulate at contact points between distinct particles, favouring liquid phase sintering [33]. The increased size of sintered agglomerates within Region B compared to Region A (Fig. 4) was due to the capability of already small amounts of melt to accelerate sintering processes [34]. For all deposits obtained from the upper superheater region, a layer with a morphology similar to Region B in Fig. 4 was observed. This morphology accounts for the bulk of the deposits.

A thin layer of small, spherical particles was seen at the outermost part of the deposit (Fig. 4C). These particles were thought to represent newly deposited material, for which the residence time in the deposit was not sufficient to undergo more pronounced sintering during boiler operation. It is not clear to what extent these spherical particles represented the actual deposit material during regular boiler operation. The boiler shut-down before the samples were taken likely affected the flue gas conditions within the convective pass of the boiler. Hence, the composition of the deposited particles may differ from that of particles deposited during regular boiler operation.

Based on the average particle size of 20 µm, the spherical particles on the outer deposit surface are intermediate-sized particles (ISP) [31].

Local enrichment in K on the outer deposit surface was seen in Fig. 4 E. The cause for this enrichment is currently unknown. A thin layer of spherical particles and local enrichment in K was seen on the outer surface of all deposits originating from the upper region of the superheater tubes.

Local enrichment in certain elements within a deposit, especially in direct vicinity to the steel, as seen in Fig. 4 D and E, can have a significant impact on deposit-induced superheater corrosion. Furthermore, changes within the local composition of the deposit affect the local melting behaviour. In an earlier study, deposit ageing mechanisms resulting in local enrichment of K and Cl have decreased the local first melting temperature of kraft recovery boiler superheater deposits toward the steel [23]. The impact of local differences in the deposit composition on the first melting temperature T_0 was studied in detail. For this, the “Type 1” deposit of Fig. 4 was divided into several sections and T_0 was calculated for each section. The local first melting temperature profile as a function of distance from the steel and the sections the deposit was divided into are shown in Fig. 5. The figure also shows the molar Cl/(Na + K), K/(Na + K) and S/(Na + K) ratios.

The local first melting temperature had its minimum in the innermost section closest to the steel, where the molar Cl/(Na + K) and K/(Na + K) ratios were the highest. Throughout the region enriched in K and Cl, local T_0 values were lower than in the three regions furthest away from the steel, which showed no local elemental enrichment and corresponded to the bulk of the deposit. As the Cl content of the deposit was below 5 wt-% on average, also enrichment in Cl, besides enrichment in K, caused a local decrease in the deposit first melting temperature [6]. The enrichment in Cl and K within the “Type 1” deposit was not thought to be exclusively caused by alkali chloride vapour transport within the already formed deposit. Some alkali chloride enrichment close to the steel likely took place during deposit build-up. However, layers of alkali chloride were seen within the Cl and K enriched region of the deposit as well, thus diffusional gas-phase transport of alkali chloride most likely contributed to the observed decrease in T_0 to some degree. The deposits of the present work were sampled after about 30 days of boiler operation. Whether alkali chloride enrichment would be similar in deposits after 12–18 months of operation, an interval typical between scheduled boiler shut-downs is unclear.

Above the region enriched in K and Cl, the deposit local T_0 and chemical composition remained fairly constant over a large region. The increased formation of alkali chloride layers within this deposit region did not cause any significant differences in the local chemical composition; thus, local T_0 values did not change significantly. Already minor variations in the local deposit composition, which are within the measurement error of the EDX analysis, result in changes in the calculated local first melting temperature of around 3 °C. Therefore, variations in the local first melting temperature of less than 5 °C were considered too small to assess whether calculated local variations in T_0 were caused by intra-depositional mechanisms altering the local deposit composition.

At the outermost layer of the deposit, the local T_0 value was the highest, despite being enriched in K. Besides K, the outermost deposit layer was also enriched in S, as seen in Fig. 5, while no enrichment in Cl was observed. An increasing K content does not affect the first melting temperature in deposits if the molar Cl/(Na + K) ratio remains below 0.015 [9], which applied to the “Type 1” deposit shown in Fig. 5. Furthermore, the simultaneous enrichment in S locally increased the molar SO_4/CO_3 ratio on the outer deposit surface, resulting in the observed increase in the local first melting temperature. These observations are in line with experimental results carried out by Frederick and Vakkilainen [15], and the general understanding of the melting behaviour of deposits formed in a kraft recovery boiler [26]. In terms of corrosiveness, the outer deposit region is of little interest due to the increased distance from the steel surface. In addition, the flue gas composition and the composition of the outermost deposit layer might have been affected by the boiler shut-down. Thus, the outermost layer of the deposit will not be discussed in any more detail within the present report.

3.3. Innermost layer enriched in S and K – “type 2” deposit

An example of a “Type 2” deposit with SEM/EDX maps highlighting the main characteristics is shown in Fig. 6.

The outer region of the “Type 2” deposits did not differ from that of the “Type 1” deposit in morphology and chemical composition and will therefore not be further discussed. However, the chemical composition of the innermost deposit region of “Type 2” deposits differed significantly from “Type 1”.

Closest to the steel the deposit was enriched in potassium and sulfur

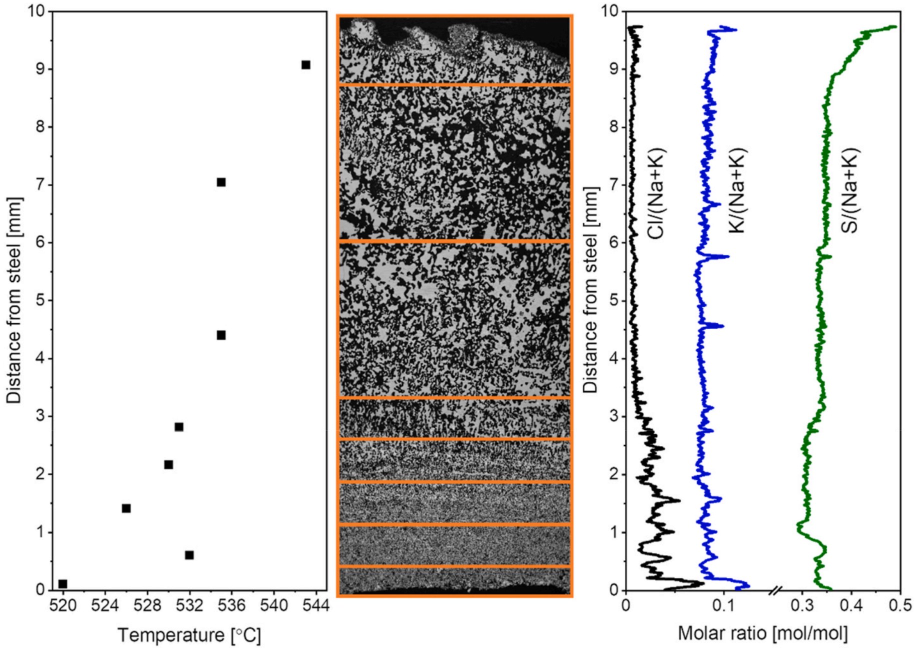

Fig. 5. Local first melting temperature of “Type 1″ deposit and molar Cl/(Na + K), K/(Na + K), and S/(Na + K) ratios as functions of distance from the steel.

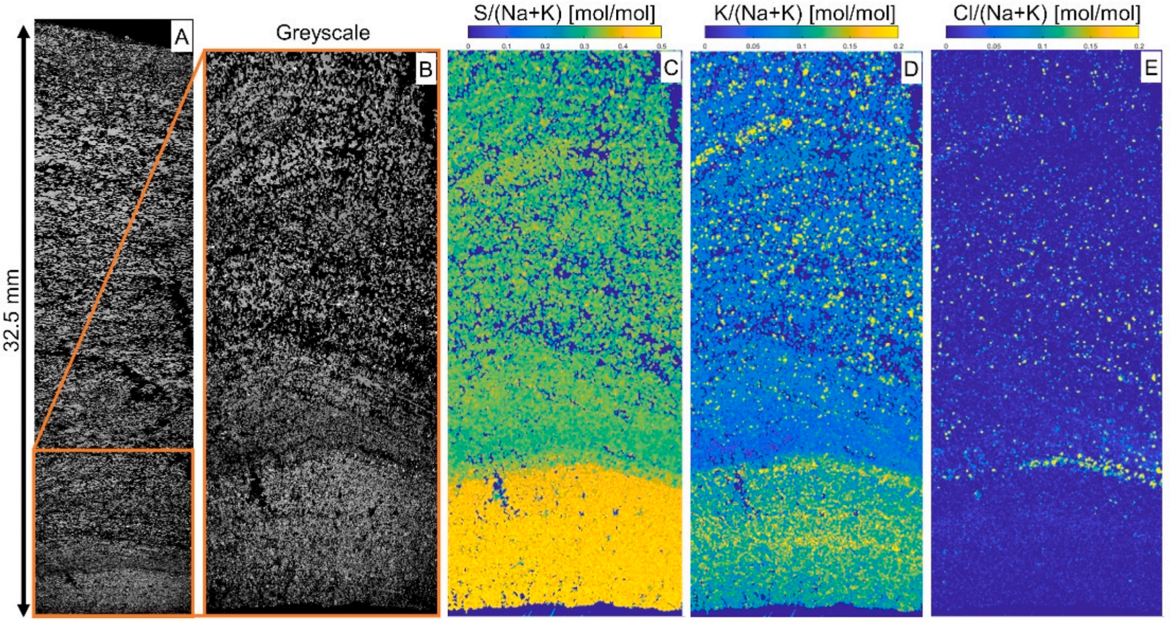

Fig. 6. A) Greyscale image of "Type 2″ deposit; B) close-up of the region closest to the steel; C) molar S/(Na + K) ratio; D) molar K/(Na + K) ratio; E) molar Cl/(Na + K) ratio.

(Fig. 6C and D), while at the same time depleted in chlorine (Fig. 6 E). The innermost region of "Type 2" deposits consisted of a dendritic structure of fine sintered particles, similar to "Type 1" deposits and was therefore believed to have formed via the same condensation mechanism.

The chemical composition of the innermost layer was believed to have formed via sulfation, whereby the initial deposit layer, originally enriched in K and Cl, reacted with SO_2 from the flue gas. Several studies in the literature have indicated that sulfation of alkali chlorides is of relevance in kraft recovery boilers [7,35] and especially toward the innermost region of deposits [7].

To further investigate whether the sulfation reaction serves as a plausible explanation for the observations made within "Type 2" deposits, the SO_2 concentration measured in the flue gas stack was analysed. Significantly higher SO_2 concentrations of 184 mg/Nm^3 on average with maximum peaks up to 690 mg/Nm^3 were recorded during the first five days of boiler operation. For the remaining operating time of the boiler, corresponding to normal operation, the measured SO_2 concentration in the flue gas stack was essentially zero. During boiler start-up, heavy fuel oil was used, known to cause higher SO_2 emissions. In addition, lower furnace temperatures during start-up as compared to normal boiler operation promoted SO_2 emission [32]. Thus, the measured SO_2 concentrations supported the hypothesis of alkali chloride sulfation to result in the analysed innermost layer composition of "Type 2" deposits.

With increasing distance from the superheater steel surface, the local chemical composition of the deposit changed. The K and S enriched region was followed by a layer enriched in Cl compared to the deposit bulk, while also slightly being enriched in K. A layer enriched in Cl but varying in thickness was analysed within all "Type 2" deposits. For the majority of samples, the Cl-enriched region did not show any enrichment or depletion in either K or S. Also, within the deposit shown in Fig. 6, the Cl-rich layer above the sulfated part of the deposit was not enriched in S, possibly due to the lack of SO_2 in the flue gas after the first five days of boiler operation. Also, regions further away from the steel had a shorter residence time in the deposit, not sufficiently long to undergo substantial sulfation.

However, sulfation of alkali chlorides alone does not explain the concurrent enrichment in K within the innermost region of the "Type 2" deposits. Currently, the K enrichment is believed to be a remnant of the initial deposit layer, originally enriched in K and Cl as seen in the "Type 1" deposit (Fig. 4). The sulfation reaction does not affect the K content within the deposit, therefore the sulfated region of the deposit remained enriched in K. However, it cannot be ruled out that some other mechanism caused the observed K enrichment. Furthermore, no definite explanation for why the S-rich layer wasn't seen within all deposit samples can be provided. Based on the analysis results, an asymmetric flue gas flow was believed to have caused local differences in the SO_2 concentration in the flue gas and therefore, not all deposit samples showed signs of sulfation. The lower boiler load during boiler start-up, compared to regular boiler operation, typically amplifies asymmetric flue gas conditions. Further research is needed to better understand the underlying mechanism(s) causing the observed local enrichment in K and S within "Type 2" deposits.

Also for the "Type 2" deposit, the local melting behaviour was analysed in more detail. The sections the deposit was divided into are shown in Fig. 7 together with the local T_0 profile and the molar K/(Na + K), Cl/(Na + K), and S/(Na + K) ratios.

The local first melting temperature within the innermost K and S enriched region of the deposit shown in Fig. 7, was increased by almost 20 °C compared to the outer deposit region, an observation made for most of the analysed "Type 2" deposits despite the locally increased K content. The local increase in T_0 resulted from the enrichment in S on one hand, and the depletion in Cl, on the other hand. These observations are in line with the general understanding of the well-studied melting behaviour of ash deposits forming in kraft recovery boilers [26]. Similar to the outer deposit surface, the local increase in the SO_4/CO_3 ratio increased T_0. Similar observations have been made by Frederick and Vakkilainen, who have identified sulfation of deposits to cause an increase in the first melting temperature [15]. In the present samples, the K increase did not affect T_0, as the molar Cl/(Na + K) ratio remained below 0.015 throughout the K-enriched region [9].

3.4. *Summary of observations and proposed deposit formation and ageing mechanisms*

The analysed deposits from the upper superheater region were classified into two main types based on differences in their chemical

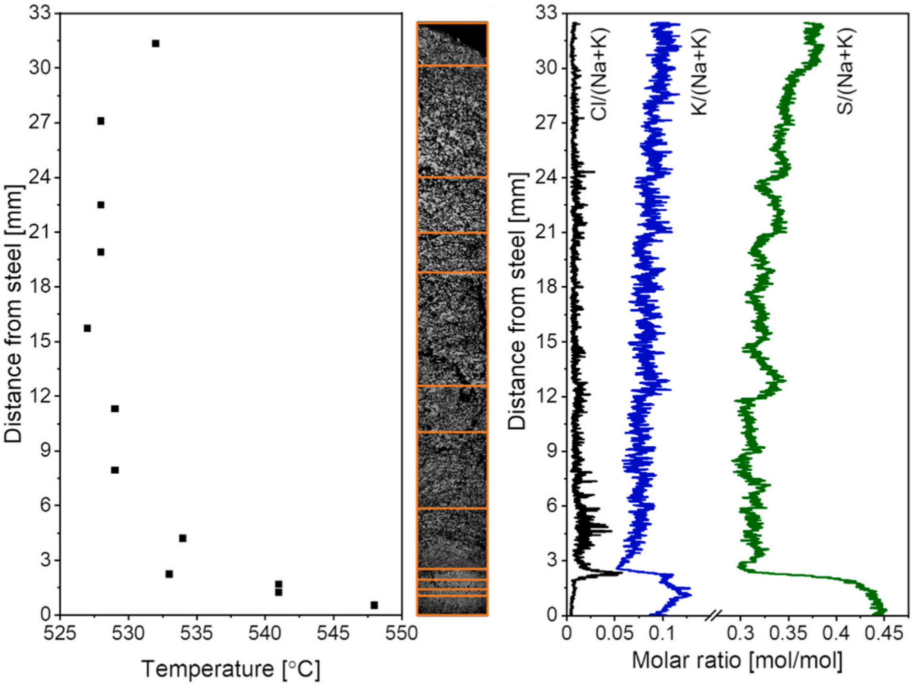

Fig. 7. Local melting behaviour and molar Cl/(Na + K), K/(Na + K), and S/(Na + K) ratios as functions of distance from the steel of innermost region of "Type 2″ deposit with locally increased T_0 close to the steel.

composition closest to the steel. In addition, some of the deposits had a morphology and chemical composition differing from these two main types. Fig. 8 summarizes all deposit types observed and puts forward an explanation for how these deposit types can be linked.

The deposits obtained from the upper superheater region were divided into two distinct regions, based on their morphological features. Closest to the steel, the deposits consisted of a porous layer of sub-micron-sized fume particles. Further away from the steel, the morphology changed to that of larger sintered agglomerates. Temperature gradient-induced diffusion of alkali chloride toward the steel was assumed the governing deposit ageing mechanism in both deposit regions.

The initial deposit layer built up as alkali chloride-rich fume particles, formed via homogeneous condensation in the flue gas, deposited on

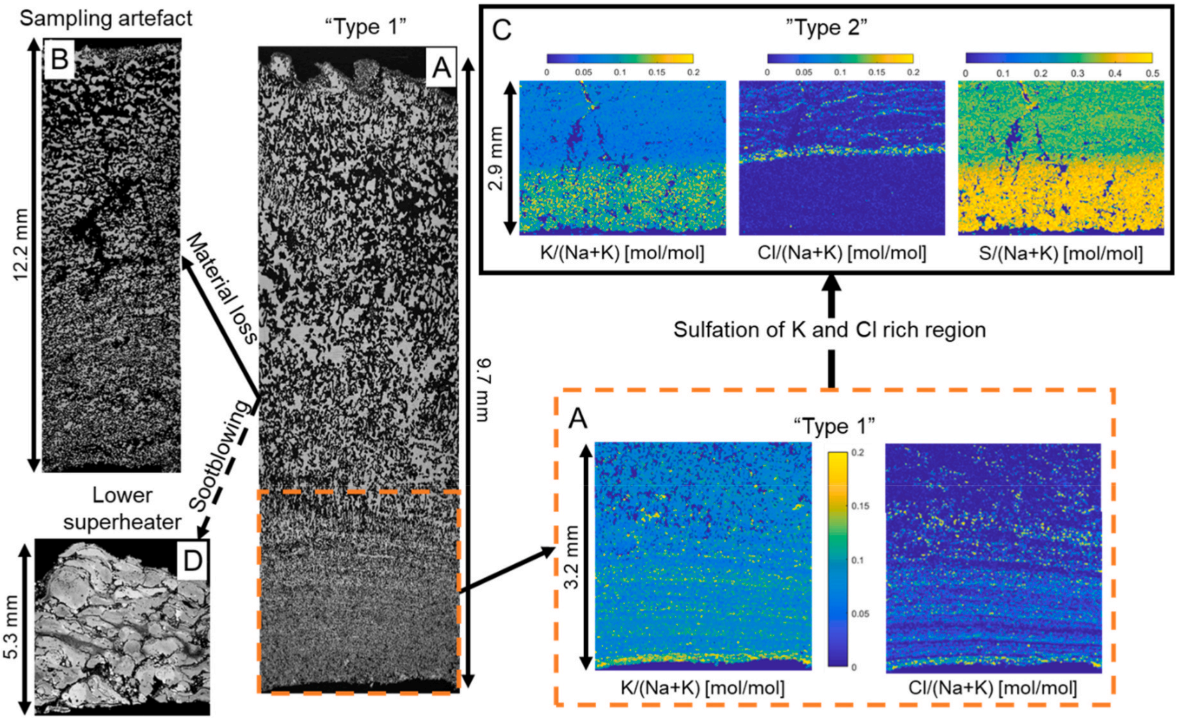

Fig. 8. Summary of identified deposit types: A) "Type 1" deposit with innermost layer of fine sintered particles enriched in K and Cl; B) Sampling artefact lacking innermost layer of fine sintered particles; C) "Type 2" deposit with innermost layer enriched in K and S while concurrently depleted in Cl; D) Thin deposit of large irregularly shaped dense particles from lower superheater region.

the superheater steel resulting in local enrichment in K and Cl closest toward the steel ("Type 1", Fig. 8 A). Local T_0 values were lower within the region enriched in K and Cl as compared to the outer regions of the deposit.

The innermost layer of "Type 1" deposits consisting of fine, sintered particles was more fragile than the outer parts of the deposit. Thus, some of the analysed samples lacked this innermost layer of fine particles (Fig. 8 B) as it presumably got lost during deposit sampling. In general, material loss during sampling could not be ruled out for any of the analysed deposit samples.

The second main deposit type had an innermost layer enriched in K and S while concurrently depleted in Cl ("Type 2", Fig. 8C), believed to have formed via sulfation of the innermost layer initially enriched in K and Cl. Local T_0 values increased within the K and S-rich layer of "Type 2" deposits due to the high S content and concurrent lack of Cl within this region.

Several deposits from the lower superheater region showed significant deviation in morphology (Fig. 8 D) compared to deposits from the upper superheater region. The underlying mechanisms causing the observed densification are currently not known.

4. Conclusions and implications

Ash deposits collected from the tertiary superheater tubes of a Finnish kraft recovery boiler were analysed regarding their chemical composition and morphology using SEM/EDX. The main findings can be summarized as the following.

- The melt fraction formed within deposits did not exceed 10 wt-%, thus the aged deposits from the upper superheater region formed a two-layered skeletal morphology. The governing deposit ageing mechanism was diffusional transport of alkali chloride vapours toward the steel, induced by the temperature gradient the deposits were exposed to.
- Type 1 deposits had an innermost layer enriched in K and Cl, formed via deposition of K and Cl-rich fume particles and additional deposit ageing. Furthermore, the local T_0 of the deposits had a minimum within the K and Cl-rich region, increasing the risk of melt formation in the direct vicinity of the steel and hampering deposit removal via sootblowing. The high Cl concentrations close to the steel and local decrease in T_0 were believed to increase the corrosiveness of the deposits.
- Type 2 deposits had an innermost layer enriched in K and S while concurrently depleted in Cl, formed via sulfation. The innermost deposit layer originally enriched in K and Cl reacted with SO_2 from the flue gas forming alkali sulfate whereas HCl was released into the gas phase. The local T_0 was shown to be increased within the sulfated region compared to the outer regions of the deposits due to the lack of Cl and concurrent increase in the SO_4/CO_3 ratio. Thus sulfation potentially reduces the risk of deposit-induced superheater corrosion.
- More research is needed to better understand the underlying cause for the observed morphological differences between deposit samples from the upper and lower superheater regions. Furthermore, a better understanding of what resulted in the concurrent presence of the two main types of deposits is needed.

CRediT author statement

Roland Balint: Investigation, Data Curation, Writing – Original Draft, Visualization. Markus Engblom: Supervision, Project administration, Writing – Review & Editing, Investigation, Validation. Jonne Niemi: Validation, Investigation, Writing – Review & Editing. Daniel Lindberg: Validation, Funding acquisition, Writing – Review & Editing. Timo Saarinen: Resources. Jaakko Rautala: Resources. Mikko Hupa: Validation, Writing – Review & Editing. Leena Hupa: Writing – Review & Editing, Funding acquisition.

Declaration of competing interest

The authors declare that they have no known competing financial interests or personal relationships that could have appeared to influence the work reported in this paper.

Data availability

Data will be made available on request.

Acknowledgements

The financing through a research grant awarded by the Fortum Foundation [Application number 20190123] is highly acknowledged. This work has been partly carried out within the Åbo Akademi CLUE^2 Research Consortium (2017–2022). Support from ANDRITZ Oy, Valmet Technologies Oy, UPM-Kymmene Oyj, Metsä Fibre Oy, and International Paper Inc. is gratefully acknowledged. Additional support from the Academy of Finland projects "Understanding the dynamics of intradeposit chemistry and morphology for control of corrosion in high temperature processes" [Decision number 310266] and "New insights on the effects of temperature gradients on high temperature corrosion" [Decision number 338322] is highly appreciated. We want to thank Linus Silvander for carrying out SEM/EDX analyses.

References

[1] Alén R. Pulp mills and wood-based biorefineries. In: Industrial biorefineries & white biotechnology. Elsevier; 2015. p. 91–126. https://doi.org/10.1016/B978-0-444-63453-5.00003-3.

[2] Vakkilainen EK. Chapter 11 recovery boiler. In: Steam generation from biomass. Elsevier; 2017. p. 237–59. https://doi.org/10.1016/B978-0-12-804389-9.00011-3.

[3] Vaahtera Eeva. Metsätilastollinen vuosikirja - Finnish statistical yearbook of forestry 2021. Helsinki: Luke Metsätilastollinen vuosikirja; 2021.

[4] Karlemo C. Non-process elements in the recovery cycle of six Finnish Kraft pulp mills. Master's Thesis. Åbo Akademi University; 2019.

[5] Tran H, Gonsko M, Mao X. Effect of composition on the first melting temperature of fireside deposits in recovery boilers. TAPPI J 1999;82:93–100.

[6] Reeve DW, Tran HN, Barham D. The effluent-free bleached kraft pulp mill - Part Xl Morphology, chemical and thermal properties of recovery boiler superheater fireside deposits, vol. 82. Pulp & Paper Canada; 1981. p. T315–20.

[7] Tran HN, Reeve DW, Barham D. formation of kraft recovery boiler superheater fireside deposits. Pulp Pap Can 1983;84:36–41.

[8] Reeve DW, Tran HN, Barham D. Superheater fireside deposits and corrosion in kraft recovery boilers. TAPPI (Tech Assoc Pulp Pap Ind) 1981;64:109–13.

[9] Tran H. Recovery boiler fireside deposits and plugging prevention, vol. 2. TAPPI Kraft Recovery Course; 2007. p. 537–72.

[10] Lindberg D, Niemi J, Engblom M, Yrjas P, Laurén T, Hupa M. Effect of temperature gradient on composition and morphology of synthetic chlorine-containing biomass boiler deposits. Fuel Process Technol 2016;141:285–98. https://doi.org/10.1016/j.fuproc.2015.10.011.

[11] Niemi J, Lindberg D, Engblom M, Hupa M. Simultaneous melt and vapor induced ash deposit aging mechanisms – mathematical model and experimental observations. Chem Eng Sci 2017;173:196–207. https://doi.org/10.1016/j.ces.2017.07.041.

[12] Niemi J, Engblom M, Laurén T, Yrjas P, Lehmusto J, Hupa M, et al. Superheater deposits and corrosion in temperature gradient – laboratory studies into effects of flue gas composition, initial deposit structure, and exposure time. Energy 2021;228. https://doi.org/10.1016/j.energy.2021.120494.

[13] Laxminarayan Y, Nair AB, Jensen PA, Wu H, Frandsen FJ, Sander B, et al. Tensile adhesion strength of biomass ash deposits: effect of the temperature gradient and ash chemistry. Energy Fuel 2018;32:4432–41. https://doi.org/10.1021/acs.energyfuels.7b03114.

[14] Skrifvars B-J, Hupa M, Hyöty P. Composition of recovery-boiler dust and its effect on sintering. TAPPI J 1991;74:185–9.

[15] Frederick WJ, Vakkilainen EK. Sintering and structure development in alkali metal salt deposits formed in kraft recovery boilers. Energy Fuel 2003;17:1501–9. https://doi.org/10.1021/ef034012s.

[16] Li X, Fakourian S, Moyer B, Wendt JOL, Fry A. Ash aerosol and deposit formation from combustion of coal and its blend with woody biomass at two combustion scales: Part 2—Tests on a 471 MWe full-scale boiler. Energy Fuel 2021;36:565–74. https://doi.org/10.1021/acs.energyfuels.1c03522.

[17] Zhang H, Yu C, Luo Z, Li Y. Investigation of ash deposition dynamic process in an industrial biomass CFB boiler burning high-alkali and low-chlorine fuel. Energies 2020;13:11. https://doi.org/10.3390/en13051092.

[18] Jensen PA, Frandsen FJ, Hansen J, Dam-Johansen K, Henrisken N, Hörlyck S. SEM investigation of superheater deposits from biomass-fired boilers. Energy Fuel 2004; 18:378–84. https://doi.org/10.1021/ef030097l.

[19] Furugaki T, Takahashi H, Hayashi S. Effect of temperature gradient in ash on high-temperature corrosion of super-heater material in a waste power generation boiler. Oxid Met 2022. https://doi.org/10.1007/s11085-022-10135-1.

[20] Costa A, Silva D, Abelha F, Cenibra CNSA. Experience of recovery boiler superheater corrosion at CENIBRA. Halifax, Canada: International Chemical Recovery Conference - ICRC; 2017.

[21] Liu X, Chen Q, Long L, Meng X, Lv G, Huang Q, et al. In-situ sampling investigation of deposition and corrosion of convective heating surfaces in a grate type municipal solid waste incineration plant: a case study. Waste Dispos Sustain Energy 2021;3:299–308. https://doi.org/10.1007/s42768-021-00087-8.

[22] Tran H, Brown CA, Jones AK. Effects of so2 on superheater fouling in kraft recovery boilers. Tappi J 2008;7:11–7.

[23] Balint R, Engblom M, Niemi J, Costa DS da, Lindberg D, Yrjas P, et al. Temperature gradient induced changes within superheater ash deposits high in chlorine. Energy 2021;226:120439. https://doi.org/10.1016/j.energy.2021.120439.

[24] Vakkilainen EK. Kraft recovery boilers - principles and practice. Suomen Soodakattilayhdistys r.y.; 2005.

[25] Bale CW, Bélisle E, Chartrand P, Decterov SA, Eriksson G, Gheribi AE, et al. FactSage thermochemical software and databases, 2010-2016. Calphad Comput Coupling Phase Diagrams Thermochem 2016;54:35–53. https://doi.org/10.1016/j.calphad.2016.05.002.

[26] Lindberg D, Backman R, Chartrand P. Thermodynamic evaluation and optimization of the (NaCl + Na2SO4+ Na2CO3+ KCl + K2SO4+ K2CO3) system. J Chem Therm 2007;39:1001–21. https://doi.org/10.1016/j.jct.2006.12.018.

[27] Laxminarayan Y. PhD thesis. In: Formation, sintering and removal of biomass ash deposits. Technical University of Denmark; 2018.

[28] Broström M, Enestam S, Backman R, Mäkelä K. Condensation in the KCl-NaCl system. Fuel Process Technol 2013;105:142–8. https://doi.org/10.1016/j.fuproc.2011.08.006.

[29] Wang Y, Tan H. Condensation of KCl(g) under varied temperature gradient. Fuel 2019;237:1141–50. https://doi.org/10.1016/j.fuel.2018.10.046.

[30] Baxter L, Hatch G, Sinquefield SA, Frederick WJ. An experimental study of the mechanisms of fine particle deposition in kraft recovery boilers. In: International chemical recovery conference. vol. 1. Charleston: Tappi Press; 2004. p. 393–412. 2004.

[31] Kochesfahani SH, Tran H, Jones AK, Grace TM, Lien SJ, Schmidl W. Particulate Formation during black liquor char bed burning. J Pulp Pap Sci 2000;26:180–7.

[32] Adams TN, Frederick WJ, Hupa M. Kraft recovery boilers. New York (NY) : Atlanta (GA): American Forest & Paper Association ; Tappi Press; 1997. 1997.

[33] German RM, Suri P, Park SJ. Review: liquid phase sintering. J Mater Sci 2009;44: 1–39. https://doi.org/10.1007/s10853-008-3008-0.

[34] Kingery WD. Densification during sintering in the presence of a liquid phase. I. Theory. J Appl Phys 1959;30:301–6. https://doi.org/10.1063/1.1735155.

[35] Boonsongsup L, Iisa K, Frederick WJ. Kinetics of the sulfation of NaCl at combustion conditions. Indus Eng Chem Res 1997;5885:4212–6. https://doi.org/10.1021/ie9603225.